A&A 412, L7–L10 (2003)
DOI: 10.1051/0004-6361:20031660

Astronomy & Astrophysics

Global sausage modes of coronal loops

V. M. Nakariakov[1], V. F. Melnikov[2,3], and V. E. Reznikova[2]

[1] Physics Department, University of Warwick, Coventry, CV4 7AL, UK
e-mail: valery@astro.warwick.ac.uk
[2] Radiophysical Research Institute (NIRFI), Nizhny Novgorod, 603950, Russia
e-mail: meln@nirfi.sci-nnov.ru, reznik@nirfi.sci-nnov.ru
[3] New Jersey Institute of Technology, Newark, NJ 07102, USA

Received 22 May 2003 / Accepted 25 October 2003

Abstract. Sufficiently thick and dense coronal loops can support global sausage magnetoacoustic modes. We demonstrate that the oscillation period of this mode, calculated in the straight cylinder approximation, is determined by the length of the loop, not by its diameter, as it was previously assumed. The existence condition for this mode is the ratio of the loop length to its diameter to be less than about a half of the square root of the density contrast ratio. This mode has a maximum of the magnetic field perturbation at the loop apex and nodes at the footpoints. We demonstrate that the 14−17 s quasi-periodic pulsations, oscillating in phase at a loop apex and at its legs, observed with the Nobeyama Radioheliograph, are interpreted in terms of the global sausage mode.

Key words. magnetohydrodynamics (MHD) – waves – Sun: activity – Sun: corona – Sun: oscillations – Sun: radio pulsations

1. Introduction

The presence of MHD wave activity in the solar corona is a commonly accepted fact. Several kinds of coronal loop wave modes have been directly observed with TRACE and SOHO spacecraft and ground-based telescopes. The particular examples are global (or standing, with the wave length equal to double the length of the loop) *kink* modes (Aschwanden et al. 1999; Nakariakov et al. 1999) and standing *longitudinal* (slow magnetoacoustic) modes (Wang et al. 2002; Ofman & Wang 2002). The particular interest to these modes is connected with MHD coronal seismology (Nakariakov et al. 1999; Nakariakov & Ofman 2001).

Another mode, the *sausage* mode, has been used to interpret periodicities in the range 0.5−5 s, which are usually observed as modulation of coronal radio emission. The estimation of the periodicity has been based upon the assumption that the period of the sausage mode is determined by the ratio of the loop cross-section radius and the Alfvén speed inside the loop (see, e.g. Eq. (2.3) of Meerson et al. 1978; Eq. (3c) of Roberts et al. 1984; Table III of Aschwanden 1987; Eq. (9) of Qin et al. 1996; Eq. (3) of Aschwanden et al. 1999; Grechnev et al. 2003). It has been pointed out by Roberts et al. (1983) (see also Edwin & Roberts 1983; and the discussion after Eq. (3c) in Roberts et al. 1984) that estimation could be used for higher spatial harmonics only. Unfortunately, the consequent papers usually did not mention this crucial restriction. Also, this estimation could not be applied to the period of *global* sausage modes.

The aim of this paper is to demonstrate that the traditionally used estimated formula for the sausage mode period is over-simplified, to give the correct estimation for the period of the global sausage mode and to illustrate this estimation by recently discovered coronal 14–17 s radio-pulsations.

2. The period of a global sausage mode

The detailed discussion and dispersion relation of sausage modes of a magnetic cylinder modelling a coronal loop, are given by Edwin & Roberts (1983) and Roberts et al. (1984). The dispersion relation clearly shows that there can *not* be trapped sausage modes in the long wave length limit $k \to 0$, where k is the longitudinal wave number. Indeed, in this case, the transverse structure of the mode outside the loop is proportional to $\exp(-m_e r)$, with m_e becoming imaginary (e.g., when $k = 0$, $m_e^2 = -\omega^2/(C_{Ae}^2 + C_{se}^2)$, where C_{Ae} and C_{se} are the Alfvén and sound speeds outside the loop, respectively). In the trapped modes, the external wave number m_e must be *real*, corresponding to the evanescent mode structure outside the loop. Thus, in the long wave length limit, there are *no* trapped sausage modes of the loop. The very existence of *non-leaky* sausage modes requires finite longitudinal wave numbers. Consequently, the estimation of the global sausage mode period P_{saus} as

$$P_{saus} = 2\pi a / C_{A0}, \quad (1)$$

where a is the loop cross-section radius and C_{A0} is the Alfvén speed inside the loop (which assumes that the wave is plane,

Send offprint requests to: V. M. Nakariakov,
e-mail: valery@astro.warwick.ac.uk

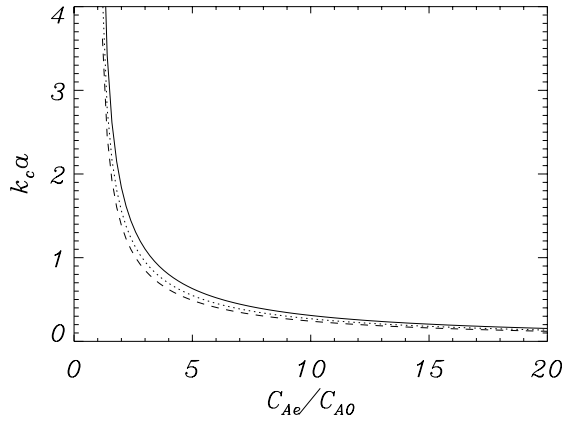

Fig. 1. Dependence of the cut-off wave number of the sausage mode upon the Alfvén speed outside the loop for different values of the internal sound speed. The wave number is measured in the loop cross-section radii a and the external Alfvén speed is measured in internal Alfvén speeds C_{A0}. The solid curve corresponds to the internal sound speed equal to $0.8C_{A0}$, the dotted curve – to $0.5C_{A0}$ and the dashed curve – to $C_{s0} = 0$.

or $k \to 0$) is *incorrect*. This expression, possibly with the change C_{A0} to kink speed C_K, can still be applied to the higher spatial sausage harmonics. However, in this case, Eq. (1) is over-simplified as it does not contain the mode number (actually, it can be correct when the mode number is exactly equal to $L/\pi a$), but does contain the kink speed which is irrelevant to the sausage mode at all.

According to Edwin & Roberts (1983), the global sausage mode exists *only* if its wave number is *greater* than a cut-off value,

$$k_c a = j_0 \left[\frac{\left(C_{s0}^2 + C_{A0}^2\right)\left(C_{Ae}^2 - C_{T0}^2\right)}{\left(C_{Ae}^2 - C_{A0}^2\right)\left(C_{Ae}^2 - C_{s0}^2\right)} \right]^{1/2}, \quad (2)$$

where C_{s0} is the sound speeds inside the loop, $j_0 \approx 2.40$ is the first zero of the Bessel function $J_0(x)$ and $C_{T0} = C_{s0}C_{A0}/(C_{s0}^2 + C_{A0}^2)^{1/2}$ is the tube speed. The cut-off wave number is shown in Fig. 1. For a significant density contrast inside and outside the loop, the cut-off wave number tends to zero for any value of the sound speed inside the loop.

The period P_{GSM} of the global sausage mode of a coronal loop is determined by the following conditions:

$$P_{GSM} = 2L/C_p, \quad (3)$$

where C_p is the phase speed of the sausage mode corresponding to the wave number $k = \pi/L$, $C_{A0} < C_p < C_{Ae}$**.** For $k \to k_c$, C_p tends to C_{Ae} from below, and for $k \to \infty$, C_p tends to C_{A0} from above. Also, the length of the loop L should be smaller than π/k_c to satisfy the condition $k > k_c$. For a strong density contrast inside and outside the loop, the period of the sausage mode satisfies the condition

$$P_{GSM} < \frac{2\pi a}{j_0 C_{A0}} \approx \frac{2.62a}{C_{A0}}, \quad (4)$$

as the longest possible period of the global sausage mode is achieved when $k = k_c$. We would like to stress that expression (4) is an *inequality*, and that the actual resonant frequency is determined by Eq. (3), provided (4) is satisfied. Combining (4) and (3), we obtain that the necessary condition for the existence of the global sausage mode is

$$L/2a < \pi C_{Ae}/2 j_0 C_{A0} \approx 0.65 \sqrt{\rho_0/\rho_e}, \quad (5)$$

so the loop should be sufficiently thick and dense.

For higher spatial harmonics of order N, expression (3) should be supplemented by an integer factor of $N > 1$ in the denominator. As the higher harmonic modes have shorter wave lengths, it is likely their wave number to be greater than the cut-off value.

3. Perturbations of the magnetic field

In the standing sausage mode of a straight magnetic cylinder, the nodes of the transverse component of the plasma velocity V_r coincide with the loop footpoints,

$$V_r \propto \sin \frac{\pi z}{L} \sin \frac{2\pi t}{P}, \quad (6)$$

where r and z are cylindrical coordinates. The small perturbation of the absolute value of the magnetic field, responsible for the modulation of the radioemission, is approximately equal to the perturbation of the longitudinal component B_z of the field. Using the induction equation, we obtain

$$|B| \propto \sin \frac{\pi z}{L} \cos \frac{2\pi t}{P}. \quad (7)$$

Thus, in the global sausage mode, the magnetic field perturbation has a maximum at the loop apex.

4. An observational example

Solar microwave bursts often display quasi-periodical pulsations with periods from ≈40 ms in narrowband bursts (Fleishman et al. 2002) up to 20 s in broadband bursts (Nakajima 1983; Stepanov et al. 1992; Qin et al. 1996; Asai et al. 2001). Broadband microwave bursts are generated by the gyrosynchrotron emission mechanism which is very sensitive to the magnetic field in the radio source. Causes of microwave flux pulsations with periods $P \approx$ 1–20 s are believed to be some kind of magnetic field oscillations that modulate the efficiency of gyrosynchrotron radiation or electron acceleration itself (see Aschwanden 1987, for a review). The observational proof of the existence of the global sausage mode should be based upon the determination of the oscillation period, the longitudinal and transverse sizes of the magnetic loop, and the spatial distribution of the oscillation amplitude along the loop. For this purpose we need a radio instrument that is able to provide us with well resolved images and a good enough time resolution. Nowadays, a necessary spatial (10″–5″) and temporal (0.1 s) resolution is provided by the Nobeyama Radioheliograph (NoRH) operating at the high microwave frequencies 17 and 34 GHz (Nakajima et al. 1994).

A good candidate for such a proof is a solar flare which happened on the 12th of January, 2000, and observed by NoRH at both frequencies. The flare had a pronounced loop-like structure well seen on Yohkoh/SXT images. Microwave and HXT images agree well with this structure.

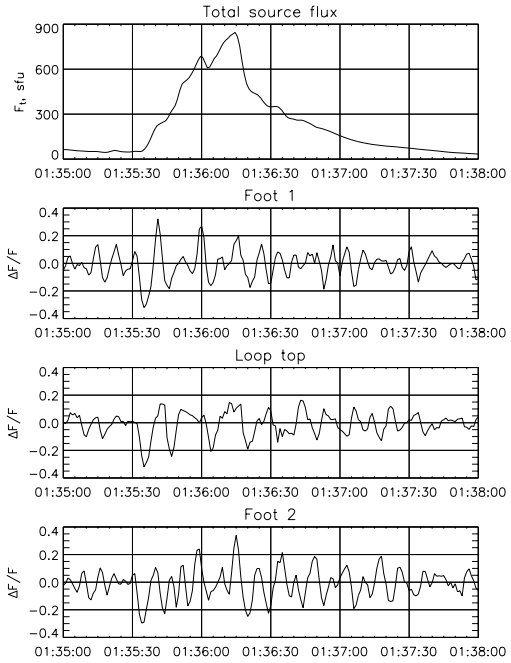

Fig. 2. First (top) panel: The time profile of the 17 GHz flux integrated over the source in the limb flare on January 12, 2000. Second to fourth panels: Radio flux variations from different parts of the flaring loop, $\Delta F/F = [F(t) - F_0]/F_0$, normalized on the slowly varying component of the emission, F_0, obtained by smoothing the observed flux $F(t)$ over 10 s. The second and fourth panels show these flux variations (quasi-periodical pulsations) as received from the $10'' \times 10''$ regions at the loop legs. The third panel shows the pulsations from the region of the same size located at the loop apex.

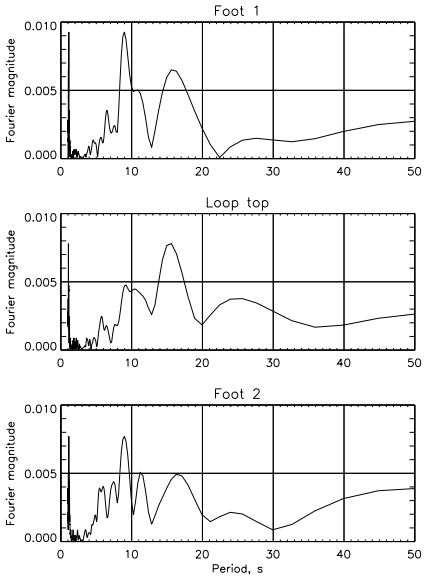

Fig. 3. Fourier power spectra of the pulsations shown in Fig. 2. Two dominant spectral components with periods $P_1 = 14-17$ s and $P_2 = 8-11$ s are clearly seen for pulsations situated at the different parts of the loop. Note that the longer period component is more intensive at the apex than in the region close to the footpoints.

Melnikov et al. (2002) found that the time profiles of the microwave emission at 17 and 34 GHz exhibit synchronous quasi-periodical variations of the intensity in different parts of the corresponding flaring loop. The length of the flaring loop is estimated as $L = 25$ Mm ($\approx 34''$) and its width at half intensity at 34 GHz as about 6 Mm ($\approx 8''$). These estimations are confirmed by Yohkoh/SXT images taken on the late phase of the flare. The loop is estimated to be filled by a dense plasma with the electron concentration $n_0 \approx 10^{17}$ m^{-3} penetrated by the magnetic field of the strength $B_0 \approx 50-100$ G. The pulsations of microwave emission flux from three boxes ($10'' \times 10''$) located at the top of the loop and at its legs are shown in Fig. 2. The corresponding Fourier spectra of the pulsations are displayed in Fig. 3. Detailed analysis of the observation and the determination of the physical parameters is given in the companion paper (Melnikov et al. 2003). Figure 3 shows that there are two main spectral components of the observed pulsations, with periods $P_1 = 14-17$ s and $P_2 = 8-11$ s. Both of them are observed everywhere in the loop. However, their relative contribution depends on the location. The first one is more pronounced at the apex while the second spectral component is relatively stronger at the loop legs. The magnitude of the first component is considerably larger at the apex than at the legs, and the opposite is true for the shorter period component. Detailed comparison of the curves in Fig. 2 shows the pulsations at the legs to be almost synchronous with the quasi-period $P_2 = 8-11$ s. At the loop apex the synchronism with the legs pulsations is not so obvious but definitely exists on the larger time scale, $P_1 = 14-17$ s. These properties of pulsations indicate the possibility of the simultaneous existence of two modes of oscillations in the loop: the global one, with the period $P_1 = 14-17$ s and the nodes at the footpoints, and the second harmonic, with $P_2 = 8-11$ s. Let us consider if physical conditions in the observed loop are consistent with the model described above.

Modelling the loop, we assume that plasma $\beta = 0$ in the external medium. In this case, the total pressure balance condition is

$$P_0 + B_0^2/8\pi = B_e^2/8\pi, \quad (8)$$

where P_0 is the gas pressure inside the loop. For following estimations, we take parameters of the flaring loop derived from microwave emission as mentioned above: $L = 25$ Mm, $2a = 6$ Mm, $B_0 = 70$ G, $n_0 = 10^{17}$ m^{-3}. Supposing the temperature inside the loop to be in the range $(5-10) \times 10^6$ K, we get the ratio between magnetic fields inside and outside the loop as $B_e \approx (1.30-1.55) \times B_0$, so they are close to each other.

We assume that the plasma concentration n_{ext} outside the loop is much less than inside, say $n_{ext} = 2 \times 10^{15}$ m^{-3}. For such values of the magnetic field and concentrations, the Alfvén speeds inside and outside the loop are estimated as $C_{A0} = 4.8 \times 10^2$ km s^{-1} and $C_{Ae} = (4.5-5.3) \times 10^3$ km s^{-1}, respectively. From expression $C_{s0} = \sqrt{(\gamma k_B T/m_p u)}$, where m_p is proton mass, k_B – Boltzmann constant, $\gamma = 5/3$, $u = 0.5$, we get the sound speed in the loop $C_{s0} = (1.8-2.6) \times 10^2$ km s^{-1}.

Substituting the characteristic speeds estimated above into Eq. (2), we get the cut-off value $k_c a = 0.25-0.28$. Thus, the longest theoretically possible wavelength λ of the trapped sausage mode of the considered loop is $\lambda \approx (22-25)a$. Consequently, as the observed loop radius is about 1/8 of its length, this loop can support the global sausage mode.

Consider now how the Alfvén speeds calculated above are consistent with the constraints derived from the other observed parameters. According to Eq. (3), for $L = 25$ Mm and $P_{\rm GSM} = 15.5$ s, the phase velocity is equal to $C_{\rm p} = 3.2 \times 10^3$ km s^{-1}. This value is close to and less than the cut-off value $C_{\rm p}(k_{\rm c}) = C_{\rm Ae}$. From Eq. (4), we get the upper limit on the Alfvén speed inside the loop: $C_{\rm A0} < 5.1 \times 10^2$ km, which is consistent with the above estimation of $C_{\rm A0}$. So, both constraints are in good agreement with the sausage mode model of the observed pulsations.

We exclude the interpretation of the observed periodicity in terms of another, kink, global mode because the value of the phase speed of this mode lies between $C_{\rm A0}$ and the kink speed $C_{\rm k}$, which for the given parameters of the loop is 665 km s^{-1}. Consequently, the period of the global kink mode is greater than 75 s, which is very far from the observed period.

Standing modes of higher harmonics have shorter wavelengths given by the expression $\lambda = 2L/N$, where $N > 1$ is an integer. The higher spatial harmonics can be responsible for the 8−11 s pulsations observed at the loop legs. However, the resonance periods of these harmonics are described by a more complicated expression, as their wave numbers are greater than the cut-off wave number and, consequently, their phase speed is *closer* to $C_{\rm A0}$ (see Melnikov et al. 2003).

5. Conclusions

We showed that sufficiently thick and dense coronal loops can support global sausage magnetoacoustic modes. The period of the oscillations is determined by the loop length and the density contrast inside and outside the loop. It contradicts the commonly used estimation for the sausage mode oscillating period as the ratio of the loop cross-section radius and the Alfvén speed inside the loop. This latter estimation is incorrect because it does not take into account the effects of external medium and the finiteness of the mode wavelength.

We demonstrated the applicability of the correct estimation for the global sausage mode period (Eq. (3)) by interpreting high spatial and temporal resolution observations of 14−17 s oscillations of coronal loops. The proposed interpretation of the 14−17 s quasi-periodic radio pulsations in terms of the global sausage mode, we believe, explains *qualitatively* all the observational findings. The further development of this topic should include taking into account the effects of the loop curvature.

Acknowledgements. The authors are grateful to Bernie Roberts and Markus Aschwanden for valuable discussions. The work was partly supported by the RFBR grants No. 01-02-16586, 02-02-39005, and NSF grant AST-0307670 and The Royal Society study visit grant 15424. VM is grateful to the National Astronomical Observatory of Japan for the support of his visit to NRO.

References

Asai, A., Shimojo, M., Isobe, H., et al. 2001, ApJ, 562, L103
Aschwanden, M. J. 1987, Sol. Phys., 111, 113
Aschwanden, M. J., Fletcher, L., Schrijver, C. J., & Alexander, D. 1999, ApJ, 520, 880
Edwin, P. M., & Roberts, B. 1983, Sol. Phys., 88, 179
Fleishman, G. D., Fu, Q. J., Huang, G.-L., Melnikov, V. F., & Wang, M. 2002, A&A, 385, 671
Grechnev, V. V., White, S. M., & Kundu, M. R. 2003, ApJ, 588, 1163
Meerson, B. I., Sasorov, P. V., & Stepanov, A. V. 1978, Sol. Phys., 58, 165
Melnikov, V. F., Reznikova, V. E., & Shibasaki, K. 2002, Proc. of Intern. Conf., Active processes on the Sun and stars, ed. V. V. Zaitsev, & L. V. Yasnov, 225
Melnikov, V. F., Reznikova, V. E., Shibasaki, K., & Nakariakov, V. M. 2003, A&A, submitted
Nakajima, H., Kosugi, T., Kai, K., & Enome, S. 1983, Nature, 305, 292
Nakajima, H., et al. 1994, The Nobeyama Radioheliograph. Proc. of the IEEE., 82, 705
Nakariakov, V. M., & Ofman, L. 2001, A&A, 372, L53
Nakariakov, V. M., Ofman, L., DeLuca, E. E., Roberts, B., & Davila, J. M. 1999, Science, 285, 862
Ofman, L., & Wang, T. J. 2002, ApJ, 580, L85
Qin, Z., Li, C., Fu, Q., & Gao, Z. 1996, Sol. Phys., 163, 383
Roberts, B., Edwin, P. M., & Benz, A. O. 1983, Nature, 305, 688
Roberts, B., Edwin, P. M., & Benz, A. O. 1984, ApJ, 279, 857
Stepanov, A. V., Urpo, S., & Zaitsev, V. V. 1992, Sol. Phys., 140, 139
Wang, T. J., Solanki, S. K., Curdt, W., Innes, D. E., & Dammasch, I. E. 2002, ApJ, 574, L101